Renewable and Sustainable Energy Reviews 226 (2026) 116338

Contents lists available at ScienceDirect

Renewable and Sustainable Energy Reviews

journal homepage: www.elsevier.com/locate/rser

Geospatial analysis of the life cycle global warming impacts from marine renewables

Tabea Engelfried, Matias Alday, Vaibhav Raghavan, George Lavidas*

Marine Renewable Energies Lab, Faculty of Civil Engineering and Geosciences, Delft University of Technology, Stevinweg, 1, Delft, 2628 CN, the Netherlands

HIGHLIGHTS

- First geospatial analysis of global warming impacts from marine renewables (MREs).
- Geospatial data are integrated into a transparent LCA for four MREs.
- Impact maps for wave energy, floating PV and floating wind in northern European waters.
- Deployment location is critical for the environmental performance of MREs.
- Not all MREs are suitable for contributing to climate change mitigation in Europe.

GRAPHICAL ABSTRACT

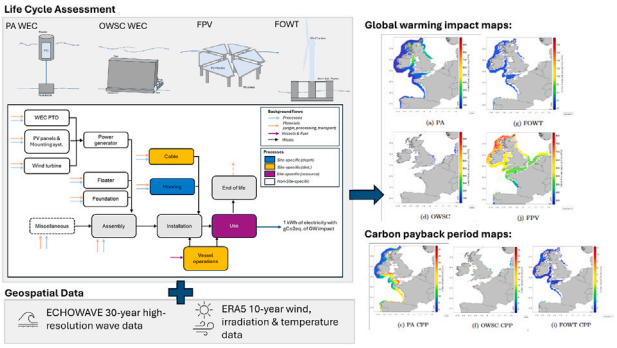

ARTICLE INFO

MSC:
0000
1111

Keywords:
Marine renewable energy
Life cycle assessment
Geospatial analysis
Climate change mitigation
Wave energy
Floating offshore PV
Floating wind turbines

ABSTRACT

The deployment of marine renewables (MRE) is important for transitioning to a low-carbon energy system. However, their performance is highly dependent on the deployment location, making the selection of feasible sites critical for large-scale implementation. To contribute meaningfully to Europe's renewable energy strategy and support a carbon-neutral energy system by 2050, the environmental performance of MREs must be taken into account in site selection, beyond the typical economic and technical aspects. Therefore, this study presents a geospatial analysis of the climate change mitigation potential of two wave energy converters, floating offshore photovoltaics, and floating wind turbines in northern European coastal waters. By combining a detailed life cycle assessment model of the four MREs with spatial data, the distribution of their life cycle global warming impact and carbon payback periods is assessed across multiple regions. The results show significantly varying impact levels of the different MREs, with carbon-neutral deployment not guaranteed at every location. Wave energy converters only partially reach carbon neutrality, while floating photovoltaics fail to do so across the entire study area. Floating wind turbines can be considered carbon-neutral nearly across their entire theoretical application area. The findings highlight the importance of taking into account site-specific environmental performance of MREs in order to ensure a positive contribution to climate change mitigation. By providing spatially explicit maps of MREs' global warming impacts and carbon payback periods, this study enables as the first of its kind the inclusion of climate change mitigation considerations in the site selection process for MREs.

* Corresponding author.
Email address: G.Lavidas@tudelft.nl (G. Lavidas).

https://doi.org/10.1016/j.rser.2025.116338
Received 17 April 2025; Received in revised form 21 August 2025; Accepted 22 September 2025
Available online 6 October 2025

Nomenclature

Abbreviations

AC	Alternating Current
AHTS	Anchor Handling & Tug Support Vessel
BEM	Boundary Element Method
BOWT	Bottom-fixed Offshore Wind Turbine
CF	Capacity Factor
CLV	Cable Lay Vessel
CPP	Carbon Payback Period
CTV	Crew Transfer Vessel
EOL	End of Life
FOWT	Floating Offshore Wind Turbine
FPV	Floating PV
GB	Great Britain
GFRP	Glass Fibre Reinforced Polymer
GW	Global Warming
HDPE	High-Density Polyethylene
HFO	Heavy Fuel Oil
LCA	Life Cycle Assessment
LCI	Life Cycle Inventory
MRE	Marine Renewable Energies
OSV	Offshore Support Vessel
OWSC	Oscillating Wave Surge Converter
PA	Point Absorber
PMSG	Permanent Magnet Synchronous Generator
PTO	Power Take-Off
PV	Photovoltaic
RP	Rated Power
WEC	Wave Energy Converter

Variables

β PV panel temperature coefficient
η Additional losses
η_{PV} Efficiency of the PV panel
A PV surface area
AEP Annual energy production
CF_{MRE} Capacity factor of an MRE
CPP Carbon payback period
D Diameter
$depth$ Water depth
$dist$ Distance to shore
$f(x)$ Probability of occurrence of x
GW Life cycle global warming impacts
$GW_{anchors}$ Life cycle global warming impacts of the anchors
GW_{cable} Life cycle global warming impacts of the export cable
$GW_{CF100,np}$ Life cycle global warming impacts of the devices in an MRE array based on a 100 % CF
GW_{chains} Life cycle global warming impacts of the mooring chains
GW_{hw} Life cycle global warming impacts of the physical export cable
$GW_{install}$ Life cycle global warming impacts of the installation of the export cable
$GW_{mooring}$ Life cycle global warming impacts of the full mooring of one device
GW_{MRE} Life cycle global warming impacts of a full MRE array with periphery at a specific location
GW_{ref} Carbon intensity of the reference electricity mix
H_s Significant wave height
Ir Incident solar irradiation
k Ross coefficient
L Lifetime
LEP Lifetime energy production
LEP_{CF100} Lifetime energy production of an MRE array based on a 100 % CF
n Number of devices
$P(x)$ Power output as function of x
P_{FOWT} Power output of a FOWT
P_{FPV} Power output of a FPV
$P_{MRE,\max}$ Maximum power output of an MRE based on its RP
P_{MRE} Power output of an MRE
P_{WEC} Power output of a WEC
RP Rated power
T Ambient temperature at 2 m above surface
t Material thickness
T_p Peak wave period
T_{panel} Panel operating temperature
T_{ref} Reference panel operating temperature
U_{100} Wind speed at 100 m above surface
x Longitude
y Latitude

1. Introduction

Anthropogenic climate change is exhibiting growing pressure on the environment and mankind [1], leading to internationally recognized commitments to work towards a carbon-neutral society by 2050 [2]. Renewable energy technology as a replacement for conventional fossil-based energy and electricity sources is seen as a necessary and highly important tool to achieve these goals [1,3–5]. Despite the agreements, rapid growth of onshore wind turbine and photovoltaic (PV) installations has recently slowed, potentially due to land use competition and social dis-acceptance [6–8]. Instead, the development of marine renewable energies (MRE) has been gaining significant momentum over the past decades. The European Union acknowledges this shift and is targeting to install marine renewables on a large scale, with 300 GW offshore wind capacity and 40 GW ocean energy planned by 2050 [9]. So far, 35 GW of predominantly bottom fixed offshore wind turbines (BOWTs) have been placed in European waters by mid-2024 [10], and floating wind turbines (FOWTs) are increasingly being developed and deployed for deeper water applications [11–13]. Additionally, offshore floating solar-photovoltaic (FPV) technology is entering the picture with recent prototype installations in the North Sea [14,15]. Furthermore, the ocean itself holds energy in the form of waves, which can be exploited by wave energy converters (WECs). This technology is potentially able to deliver more than the current global annual electricity demand [16]. In addition, the resource's lower seasonal variations, predictability, and different intermittency patterns compared to wind and solar [16–18] are suspected to make WECs suitable components for diverse and secure renewable-based electricity grids [19].

For MREs, the deployment location determines technically and economically feasible deployment [20–22], which is crucial for large-scale implementation. The local resource like the wave energy flux, wind speed, or solar irradiation, and its characteristics, defines patterns and magnitude of electricity production [23]. In addition, environmental conditions affect a device's survivability, therefore structural requirements, and risk of damage [24,25]. Water depth and distance to coast affect installation and maintenance, driving cost and material requirements of moorings and grid connection [26,27]. Wind, wave, and tidal climate conditions, directly impact the performance, influence weather windows, and therefore are a major factor for device availability [24]. This multilevel interaction between location- and performance parameters of the installation makes site selection for MREs a complex process, already excluding limitations imposed by other sea users and marine spatial planning.

In this context, many researchers performed geospatial analysis on factors for successful MRE implementation on varying geographical scopes. Gunn & Stock-Williams [28] and Guillou et al. [29] map global and local theoretical resource-based potentials for wave energy. Soares et al. [30] and Zheng et al. [31] do so for offshore wind, and Silalahi et al. [32] for solar energy. Weiss et al. [20] and Guillou et al. [33] assess the deployment potential of WECs and wind turbines, considering geographical constraints implied by logistics for installation and maintenance, as well as possible grid connection. Other studies map the spatial distribution of economic potential of WECs [16,27,34], FPV [26], BOWTs [35] and FOWTs [25]. Lavidas [36] analyses the overall performance of WECs in the North Sea area based on three pillars, namely resource potential, energy extraction potential, and economics. Furthermore, various studies develop criteria and methods for selecting feasible sites based on different performance parameters [37–41].

However, an important parameter that is missing in these geospatial performance assessments is the environmental impact of the installations, although it is also strongly dependent on the site. Given that, in addition to economically and technically feasible solutions, energy technologies with a proven low global warming (GW) impact are needed to meet set climate targets and contribute to climate change mitigation, this highlights a significant gap in the literature on MREs. An approach that can be used to determine environmental impacts of MREs is life cycle assessment (LCA). LCA is a method to quantitatively assess the potential environmental impacts a product is associated with over its entire life cycle [42].

A number of LCA studies on specific MRE prototypes and at specific deployment locations have been performed. For wave energy converters, GW impacts in a range of 20 to 374 $gCO_2eq./kWh$ have been found in 20 studies performed until 2024 [43,44]. The most comprehensive LCAs on WECs to date are from Thomson et al. [45] (Pelamis attenuator), Pennock et al. [46] (CorPower point absorber (PA) array), Apolónia & Simas [47] (MegaRoller oscillating wave surge converter (OWSC)), and Engelfried et al. [44] (representative PA), which are mostly methodologically consistent cradle-to-grave studies that assess a wide range of impact categories according to mature impact assessment methods. The most dominant conclusions are that structural materials account for the majority of environmental impacts, followed by vessels for installation, operation and maintenance [43]. Recently, Engelfried et al. found that the electrical cable can also have large influence on the results, depending on the installation's distance to shore [44].

For the more mature BOWTs, numerous LCAs are available and converging values revolving around 20 $gCO_2eq./kWh$ are established [48–51]. However, studies including more accurate data on maintenance, repairs and spare parts present higher results up to 43 $gCO_2eq./kWh$ [52]. For different types of FOWTs, GW impacts in a similar range of 17 to 45 $gCO_2eq./kWh$ are found [53–57]. The upper limit is a result by Garcia-Teruel et al. [58], who present a comprehensive study on a semi-submersible and spar buoy FOWT, also including improved assumptions on maintenance and spare parts. For FPVs, only one LCA study by Clemons et al. [59] is known to the authors, finding GW impacts of 73.3 $gCO_2eq./kWh$ for an HDPE-Pontoon FPV plant for sheltered waters in Thailand.

For wind energy, additional studies assess the life cycle environmental impacts of the technology in a wider spatial context. Tsai et al. [21], Pulselli et al. [60], and Poujol et al. [54] perform LCAs on bottom fixed and floating turbines at several locations in the Great Lakes, Mediterranean, and North Atlantic respectively. They present a significant location dependence of results through resource variations, larger distances to shore, and water depth. Also, Blanc et al. [22] highlight the importance of geographical data on LCA results of renewables in a unique effort to combine geospatial analysis of the offshore wind resource and life cycle assessment within the EnerGEO project [61]. The study presents GW impacts of 13 to 23 $gCO_2eq./kWh$ for a wind farm of 30 5 MW turbines, placed all across the North Sea. They consider local resource data, a water depth dependent foundation (bottom fixed tripod or floating), as well as transmission cable length and vessel efforts based on distance to shore.

With the exception of the small number of studies on offshore wind energy described above, LCAs on MREs miss the spatial aspects of environmental performance. However, to enable and encourage consideration of this important factor in decision making and site selection, spatially dependent GW impacts of MREs need to be made explicit.

This study, therefore, aims to contribute to the body of literature by presenting a detailed analysis of the geospatial distribution of life cycle GW impacts of MREs. A uniquely adaptable and transparent life cycle inventory (LCI) of four different generic MRE devices, with potential relevance for large-scale application in European waters, is also provided. Covered MREs are the two most far developed WEC types PAs and OWSC, as well as FPV, and FOWTs. BOWTs are excluded due to more mature already existent literature [22,62]. The LCA in this study builds upon a recently proposed approach for a representative LCI for a generic PA WEC [44], which is expanded to include more MRE technologies. The obtained GW impacts are coupled with spatial resource data for North Atlantic and North Sea European coastal waters, to assess the spatially dependent climate change mitigation potential of the MREs. By providing fully disclosed, technology-representative LCI data, this study overcomes the limitations of the majority of previous MRE LCAs, which focused on commercially proprietary, specific devices and thus made it difficult to draw broader conclusions about the technology's performance. By including geospatial analysis in the LCA, this study enables, as the first of its kind, the inclusion of climate change mitigation considerations in the site selection process for MREs.

The paper is structured as follows: In Section 2, the methods used to obtain the spatially dependent GW impacts for the four MREs are explained. In Section 3, the obtained impact maps are presented. The findings are discussed in Section 4, and the main conclusions and recommendations are summarised in Section 5.

2. Methods

To obtain the geospatial distribution of MRE environmental impacts, data on resource and location parameters within the area of interest are coupled with an attributional LCA of the MRE devices. This section describes the studied MRE archetypes, their performance evaluation, the LCA's underlying assumptions, origin and use of spatial data, as well as the combination of these components towards impact maps for each technology (see Fig. 1).

2.1. Technology archetypes

As proposed by Engelfried et al. [44], the modelling of the MREs follows their modular structure. The MRE archetypes are divided into systematic function groups, similar across the five technologies: the power generator, the floater, the foundation, and the mooring. Major components of the archetypes are defined for each technology, and do not differ significantly across developers, hence they are considered generic. Information has been aggregated from different far developed prototypes of each technology. The referenced prototypes are referred to as sources in Table 1. Where parts of the LCI have been adapted from other sources, system boundaries for the foreground system were kept comparable between technologies, and overarching materials for the major functional components and representative background processes for major processing steps. For the FPV, the power generator (PV cells) is used from ecoinvent as the available dataset is considered to be consistent with these boundaries. The LCA product system will be structured based on this categorisation. The modelled device configurations are summarised in Table 1 and visualized in Fig. 2. Detailed underlying assumptions, data sources, dimensions, and material compositions of components can be found in the supplementary material.

The floaters consist of hot rolled low-alloyed steel plates of the given thickness (t). Further, a low to medium voltage transformer, control

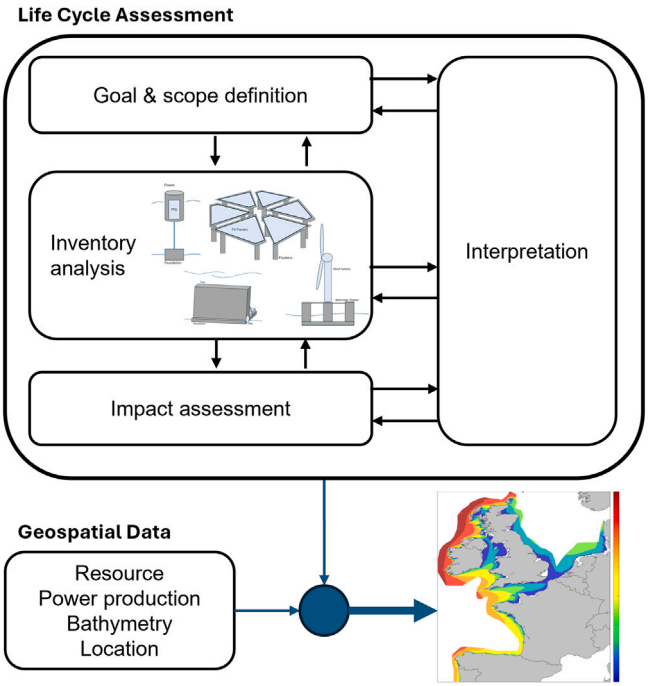

Fig. 1. Overview of the study structure.

units, and anti-corrosive glass flake paint for the hull are considered. All devices are assumed to have a lifetime of 20 years. For grid connection, a 33 kV AC 3-core copper conductor electrical transmission cable (same for all devices) is used. As elaborated in [44], the cable system for the high-level analysis is not specifiable, and an average of the material compositions for medium voltage submarine cable types most commonly used according to mechanical-, cost-, and loss-properties is taken [77–79]. Due to this reason, the varying cable length and unknown environmental conditions within the analysis, transmission losses are omitted.

For the five MRE technologies, devices are assessed as grid-connected arrays. The number of devices in an array is based on their single rated powers and the power transmission capacity of one export cable (25 MW), including a safety margin. Due to the high-level analysis, no array- and inter-array cable layout is defined. Each device uses its own mooring, as potential designs for mooring sharing are not well established yet [80,81].

2.2. Spatial data and power production estimation

The study's area of interest for the spatial distribution of MRE's GW impacts is European coastal waters within 200 km of shore in the North Atlantic and North Sea. Applicable deployment areas are limited by the water depth range specified for each technology, with a maximum of 200 m. Bathymetry data is sourced from GEBCO [82]. For the visualization, coastline data has been obtained from Wessel et al. [83]. Fig. 3 shows the water depth and distance to shore in the studied area.

To obtain the power output of the MRE arrays, different methods based on the specific technology were applied. Resource data for WEC power output estimations is sourced from the ECHOWAVE hindcast, which contains wave parameters and spectral data from over 30 years (1992–2021) in a ~2,3 km resolution [84,85]. Power matrices, which describe the power production of the WEC in each sea state (see Fig. 4), were obtained using a weakly non-linear boundary element formulation, and were developed utilizing the open-source BEM solver HAMS-MREL [86]. The power matrix is constructed considering irregular sea states based on the JONSWAP spectrum for the power calculation [86]. The defined depth restrictions are based on the power matrix applicability. The WECs' average output power at a location is calculated by combining the power matrix $P(H_s^i, T_p^j)$ and the local 30-year average probability of occurrence $f(H_s^i, T_p^j)(x, y)$ of significant wave heights H_s and peak wave periods T_p (Eq. (1)).

$$P_{WEC}(x,y) = \sum_{i=1}^{n_{H_s}} \sum_{j=1}^{n_{T_p}} P(H_s, T_p) \cdot f(H_s^i, T_p^j)(x,y) \tag{1}$$

For the FPV and FOWT, 10-year (2012–2022) ERA5 data with a ~30 km resolution for the same area is used [87]. The power output of the PV panels at a location is calculated using the local 10-year average solar irradiation reaching the horizontal plane (Ir) over the PV surface of the FPV plant (A) (Eq. (3)). A de-rating factor of $\eta = 0.85$ accounts for effects of soiling, ageing, and electrical losses [26,88]. In addition, changes in panel efficiency due to deviations in panel temperature from the reference temperature ($T_{ref} = 25°C$) are included. The panel temperature is calculated based on the Ross coefficient $k = 0.025$ for free standing modules [89,90] and 2 m above surface ambient temperature (T) [91] (Eq. (2)). The panel conversion efficiency $\eta_{PV} = 0.22$ and temperature coefficient $\beta = 0.003$ have been obtained from manufacturer data sheets of 680 Wp mono-crystalline panels [92–95].

$$T_{panel}(x,y) = T(x,y) + k \cdot Ir(x,y) \tag{2}$$

$$P_{FPV}(x,y) = Ir(x,y) \cdot A \cdot \eta_{PV} \cdot (1 - \beta \cdot (T_{panel}(x,y) - T_{ref})) \cdot \eta \tag{3}$$

For FOWTs, turbine power output is determined by combining the geographically specific average wind speed at 100 m above surface (close

Table 1
Modelled MRE archetypes.

	Floater	Power generator	Foundation	Mooring	Applicable depth
PA WEC	D9x18 m, t50 mm Cylinder	600 kW Linear generator	40 t Steel vertical anchor	Tension rod towards foundation	50–200 m
Sources	[44,63,64]	[44,65]	[66]	[64]	
OWSC WEC	26x10x4,7 m, t45 mm Rectangular flap	1000 kW Hydraulic power-take off (PTO)	28x4x11 m Reinforced concrete foundation	4-line flat mooring 50 kg/m, ~50 mm, chains Line length constant 130 m along the seabed 5 t concrete gravity anchors	13–20 m
Sources	[47]	[45,67,68]	[47]	[47,69,70]	
FPV	18 D3,2x10 m, t20 mm Cylindrical piles	500 kWp 2400 m2 PV surface 680 Wp mono-crystalline panels	No foundation	6-line spread catenary mooring 50 kg/m, ~50 mm chains, Line length 5,5 times water depth 15 t drag embedment anchors	20–200 m
Sources	[71]	[71]		[69–73]	
FOWT	3 D13x35 m, t30 mm Cylindrical main piles	9500 kW 3-bladed offshore wind turbine Geared PMSG	No foundation	4-line spread catenary mooring 400 kg/m, ~140 mm chains, Line length 8 times water depth 20 t drag embedment anchors	60–200 m
Sources	[74]	[58]		[58,74–76]	

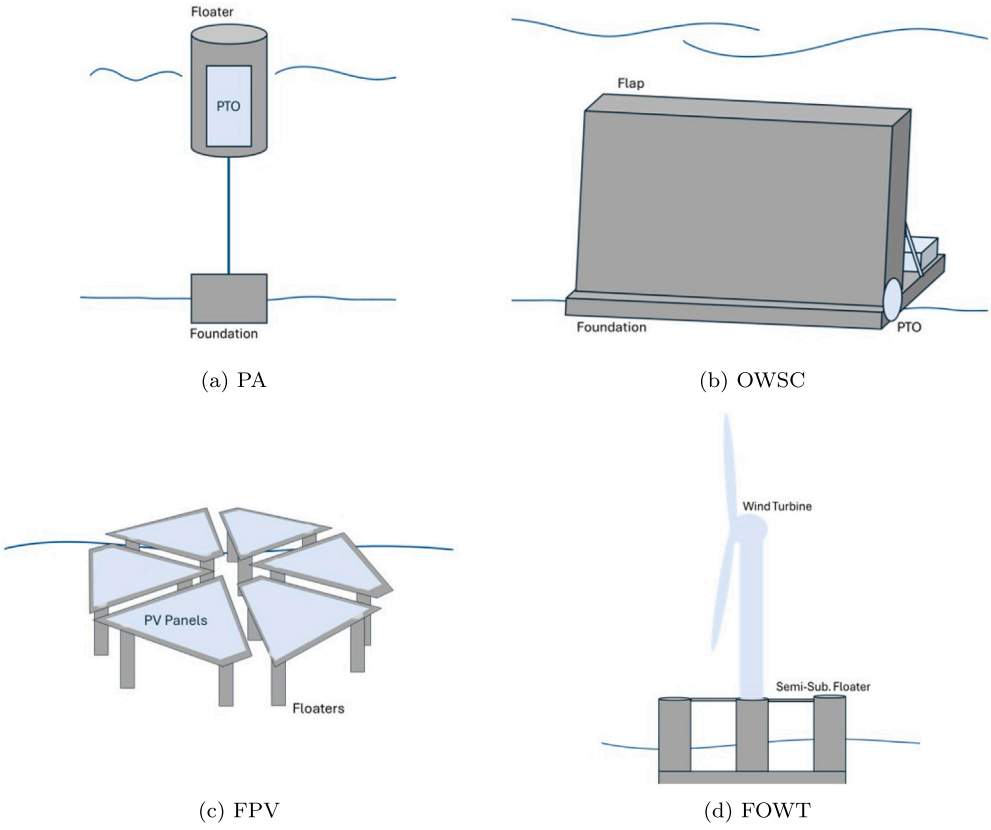

(a) PA (b) OWSC

(c) FPV (d) FOWT

Fig. 2. Modular structure of modelled MRE archetypes.

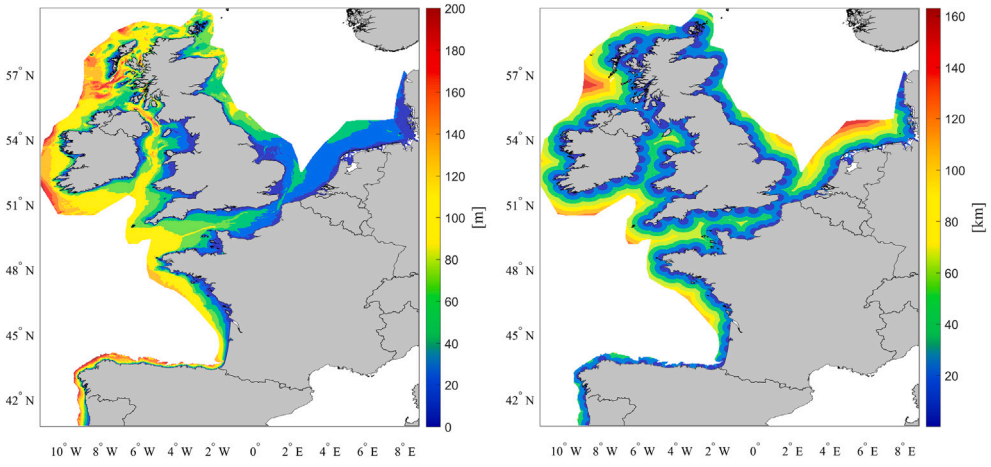

(a) Water depth (b) Distance to shore

Fig. 3. Location parameters water depth and distance to shore in the studied area.

to hub height) U_{100} and the power curve for the DTU 10 MW reference turbine $P(U_{100})$ [96] (Eq. (4)). Electrical and heat losses as well as degradation are accounted for with an aggregated η of 95 % according to [25].

$$P_{FOWT}(x,y) = P(U_{100}) \cdot U_{100}(x,y) \cdot \eta \tag{4}$$

The resource characteristics at one grid point are later fed into the LCA model summarised as the resulting average capacity factor (CF) over the temporal domain of the underlying dataset (Fig. 5). The CFs are calculated using the MRE's maximum power output $P_{MRE,\max}$ based on the rated power (RP), and the average resource-driven power output at the specific location P_{MRE} (Eq. (5)).

In this study, array effects are not accounted for, making the CF of a single device equal to that of the array. For WECs, inter-device spacing in the array is assumed to be wide enough so that negative device interactions are no longer expected [97].

$$CF_{MRE}(x,y) = \frac{P_{MRE}(x,y)}{P_{MRE,\max}} \tag{5}$$

For both WECs, CFs are highest in areas not shaded from waves by landmasses. The PA and OWSC achieve maximum CFs of 36 % and 39 %

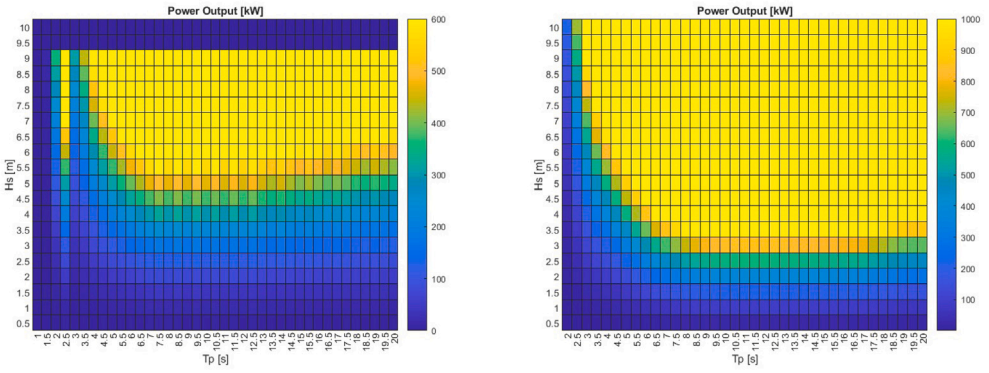

(a) PA (b) OWSC

Fig. 4. Power matrices of assessed WECs.

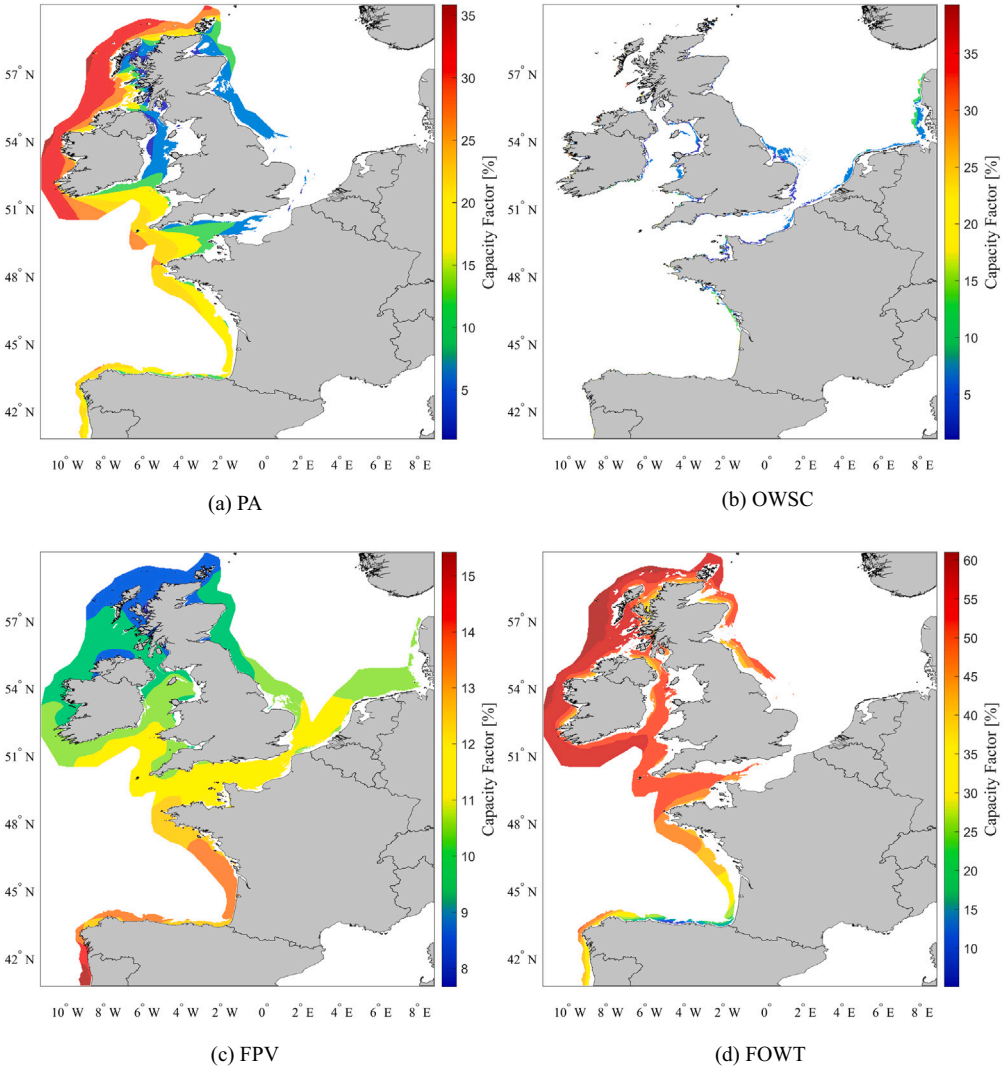

(a) PA (b) OWSC

(c) FPV (d) FOWT

Fig. 5. CFs of the studied MREs in their applicable area of deployment.

at the west coast of Ireland and Scotland close to shore, and with the maximum possible distance from shore within the applicable area, respectively. While the PA has larger areas with CFs in the upper regions of the full range, the OWSC presents high CFs only in very few locations. In the majority of areas lower CFs of around 10 % and less are found. The FPVs' CF is decreasing with latitude, reaching a maximum of 15 % at the coast of Portugal, and a minimum of 8 % north of Scotland. FOWTs' CFs are more constant across the area, with only a slight increase with

latitude and distance to shore up to a CF of 61 % west and north of Scotland and Ireland can be observed. Lowest CFs of 10 to 30 % are achieved in the southern Bay of Biscay.

2.3. Life cycle assessment modelling

To determine the MRE's potential life cycle impacts on climate change, a cradle-to-grave attributional LCA model has been created, including the manufacturing & assembly, installation, use, and end of life (EOL) phases. The principal product system is provided in Fig. 6. It is constructed based on the devices' functional groups explained in Section 2.1. Dependencies of different parts of the product system on the deployment location are highlighted.

Climate change impacts from an MRE are assessed for a functional unit of 1 kWh of electricity delivered to the onshore grid. The global warming potential over a 100-year time horizon [98] as defined in the environmental footprint method EF 3.1 provided by the European Union [99], is used as assessment method for determining climate change impacts. The impact calculations and life cycle modelling are executed in openLCA [100]. Background data are sourced from the ecoinvent 3.10. cut-off by allocation database [101].

The structure and framework behind the LCIs for the presented MREs largely follow the representative LCI for a generic PA WEC presented by Engelfried et al. [44]. The outlined approach has been extended to the FPV as well as the FOWT. As the method is previously described in detail, only the changes made for this study are explained.

For the power generator of the FOWT - the wind turbine (tower, generator, blades) - LCI data from Garcia-Teruel et al. [58] has been adopted. For the PV panels and mounting structure, ecoinvent datasets are utilized [102,103]. The average material composition of the cable has been derived from Arvesen et al. [52], which provides information on the material compositions of five different medium-voltage copper conductor cables with different cross-sectional areas currently available on the market. Detailed information on all underlying assumptions regarding material compositions, processing, transport, applicable background datasets as well as the full LCI for all MREs can be found in the supplementary material.

2.3.1. Manufacturing & assembly

The devices are assembled from the hull materials (hot rolled steel plates), and coupled with major pre-manufactured components (control, transformer, paint, and power generator) at an assembly site at a port close to the deployment location. Predominantly manual labour is assumed, except for lift operations with a diesel-powered crane. Exemplary processing of materials (metal working from raw to semi-finished product) is included for all large material inputs. Welding is excluded. For the FOWT, coupling of the floater and the turbine is assumed to also take place at the port site, eliminating the need for offshore heavy lift vessels at the later installation [104]. The inclusion of transport and applicable geographies for background data is modelled as outlined in [44].

2.3.2. Offshore activities

Installation, maintenance, and decommissioning of MRE devices rely on offshore vessel operations. For representation of these in the LCA, first, the total fuel requirement is obtained by coupling activity durations with the hourly fuel consumption of used vessels. The vessel use is then represented by the ecoinvent ferry (large, heavy, vessels propelled by heavy fuel oil (HFO)) and barge (small, fast, diesel propelled vessel) by scaling their fuel consumption to the activities' reference unit of transported tonne kilometres [44]. Table 2 presents all considered activities, durations, and vessels based on those presented in Engelfried et al. [44]. Adjustments for FOWTs and FPVs have been made where necessary due to the larger dimensions and differences in moorings. Vessel fuel consumptions shown in Engelfried et al. [44] are used unchanged.

2.3.3. Use phase

During the use phase, the MRE array produces electricity without any direct emissions related to the power conversion. Only a part of the MRE array can be attributed to the production of 1 kWh of electricity. Therefore, the LCI is scaled by lifetime energy production (LEP) as shown in Eqs. (6)–(8). The equation holds for both a single MRE device and an array of the size $n > 1$.

$$AEP\ [kWh/yr] = n\ \cdot RP\ [kW] \cdot CF\ \cdot 8760\ h/yr \tag{6}$$

$$LEP\ [kWh/device] = AEP\ [kWh/yr] \cdot L\ [yr/device] \tag{7}$$

$$Inventory\ [1/kWh] = \frac{Inventory\ of\ Inputs\ [1/device]}{LEP\ [kWh/device]} + \frac{Inventory\ of\ outputs\ [1/device]}{LEP\ [kWh/device]} \tag{8}$$

During the lifetime of the devices maintenance is required. A baseline scenario of annual inspections for small repairs and preventive maintenance, as well as tow-backs for larger corrective maintenance of each device once every four years is considered [44]. In an array, every device gets towed to shore at the specified interval, and inspections take place for all devices within one visit of the CTV. Spare parts, energy and material inputs for repairs, as well as effects of downtime on electricity production, are excluded from this high-level analysis. Proven maintenance strategies and publicly available data for MREs are to a varying degree between technologies still uncertain, especially for WECs [109,110] and FPV [111]. For offshore wind turbines more quantitative

Table 2
Offshore vessel activities during MRE device installation, maintenance and decommissioning.

Phase	Activity	Duration	Vessels[1]	Source
Cable installation	Laying and burying	3,5 h/km	CLV	[79]
Site preparation	Preparation and mooring pre-lay (Flat mooring)	12 h	AHTS, OSV	[68,105,106]
Site preparation	Additional time per line for catenary moorings	12 h	AHTS, OSV	[76]
Site preparation	Foundation installation (PA)	13 h	OSV	[46]
Transit	Towing floater to site	0,1 h/km	Tug	[46,105–107]
Connection	General time for cable connection, placing of device	8 h	AHTS	[46,68,105,108]
Connection	Additional time per line for catenary moorings	8 h	AHTS, OSV	[76]
Maintenance inspections	Transit	0,03 h/km	CTV	
Maintenance inspections	Stationary per device	6 h	CTV	
Maintenance tow-backs	Disconnecting (reversed connection)	See connection		
Maintenance tow-backs	Towing from and to site	See transit		
Maintenance tow-backs	Connecting	See connection		
Decommissioning	Disconnecting (reversed connection)	See connection		
Decommissioning	Towing from site	See transit		
Decommissioning	Removal of moorings (reversed preparation)	See site preparation		

[1] CLV = Cable Lay Vessel, AHTS = Anchor Handling and Tug Support Vessel, OSV = Offshore Support Vessel, HFO propelled; CTV = Crew Transfer Vessel, diesel propelled

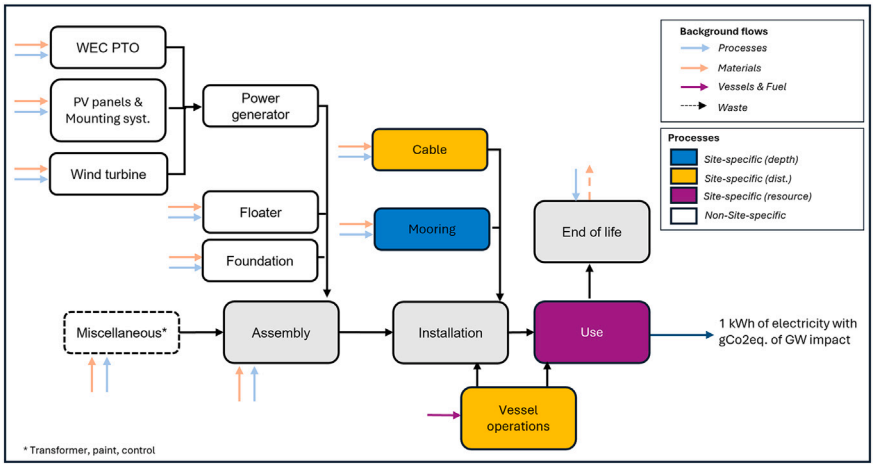

Fig. 6. Simplified representation of the product system for the MRE devices with different applicable power generators and indication of dependencies on the location.

information on maintenance strategies is available [52,58], however, to maintain a comparable level of fidelity within the MREs of this study the maintenance assumptions are assumed to be consistent for all considered MRE devices.

2.3.4. End of life

At their EOL the MRE devices, moorings, and foundations are assumed to be removed, and the materials are recovered for EOL treatment or recycling. Removal and transport of the devices back to shore are modelled as the reversed installation, as described in Section 2.3.2. The transmission cable is left in the ground and materials are not recovered [75,112,113].

Energy and process inputs for the dismantling are assumed to be the same as for the assembly stage. The regained materials are assumed to be partially recycled according to the assumptions in Engelfried et al. [44], and partially disposed of according to the disposal pathways used in ecoinvent waste markets (mostly landfilling and forms of incineration). The GFRP turbine blades are disposed of as waste glass and plastic mixture [114]. Also for the PV panels, the proposed material shares and disposal pathways of the ecoinvent source dataset have been adopted [102].

For consistency with the chosen ecoinvent system model, the cut-off allocation method is applied. EOL recycling processes are therefore considered to be outside the system boundary, and no recycling credits are given. The recycled material contents (90 % steel and 60 % copper [45,115]) therefore only reduce the amount of material that is, e.g., incinerated or landfilled otherwise.

2.4. Geospatial and LCA data aggregation

As shown in Fig. 6, some parts of the LCI depend on site-specific parameters. The LCA model is therefore coupled with resource and bathymetry data, to assess the spatial distribution of GW impacts of MRE devices.

To combine the LCA and spatial data, location-independent GW results are extracted from openLCA. These are then post-processed with the resource and location parameters. This approach is used to minimize computational effort within openLCA which is not built to run large amounts of “scenarios”, with each scenario representing a grid point within the studied area. The applied procedure is visualized in Fig. 7.

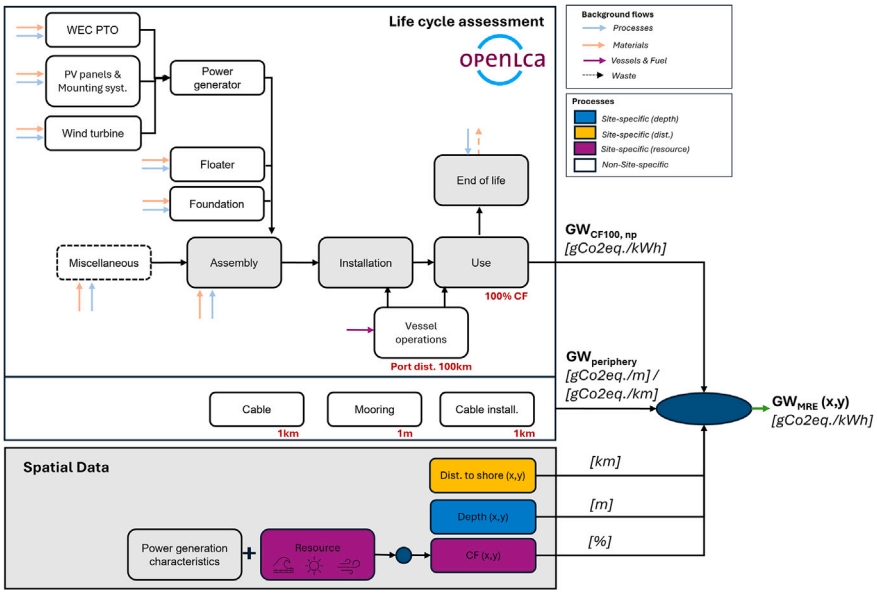

Fig. 7. Approach for combining spatial data and GW impacts obtained in openLCA.

Location-independent GW results for an MRE $GW_{CF100,np}$ are calculated in openLCA with an assumed 100 % capacity factor, and without periphery (cable and mooring) that depend on distance $dist$ to shore and $depth$. As the CF scales all parts of the inventory equally (see Eq. (8)), the CF100-result can later be corrected with the location-specific CF $CF_{MRE}(x,y)$ by division, to obtain the overall array result GW_{MRE} (see Eq. (11)). To include the array periphery, GW results for a device mooring at 1 m water depth ($GW_{chains}, GW_{anchors}$), and 1 km of cable hardware GW_{hw}, as well as its installation $GW_{install}$ are extracted from openLCA and related to 1 kWh of electricity produced by division with the LEP based on a 100 % CF LEP_{CF100}. The combined location-specific GW impact per kWh of electricity produced by the array with periphery is calculated as shown in Eqs. (9)–(11).

$$GW_{cable}(x,y)\ [gCo2eq./kWh] = \frac{(GW_{hw} + GW_{install}\ [gCo2eq./km]) \cdot dist(x,y)[km]}{LEP_{CF100}[kWh]} \quad (9)$$

$$GW_{mooring}(x,y)\ [gCo2eq./kWh] = \frac{GW_{chains}\ [gCo2eq./m] \cdot depth(x,y)\ [m] + GW_{anchors}\ [gCo2eq.]}{LEP_{CF100}[kWh]} \quad (10)$$

$$GW_{MRE}(x,y) = \frac{GW_{cable}(x,y) + n(GW_{mooring}(x,y)) + GW_{CF100,np}}{CF_{MRE}(x,y)} \quad (11)$$

In contrast to the cable length and laying operations, vessel operations depend on the distance to the nearest port rather than on the distance to shore. However, this parameter can't be expressed in terms of distance to shore as the choice of supply port is dependent on more economic and strategic factors [107,116]. Therefore, an assumed constant distance to port of 100 km for installation and maintenance activities is applied for the whole area.

Finally, each device's carbon payback period (CPP) across the area of interest (Eq. (12)) is calculated. This indicates how long it will take for the MRE array to offset its life cycle embedded carbon by displacing other electricity sources with potentially larger impacts [117] and become carbon-neutral. The reference value (GW_{ref}), which is assumed to be offset in this analysis, is 258 $gCO_2eq./kWh$, the average carbon intensity of the European Union's electricity mix in 2022 [118]. The CPP is used as an indication of the climate change mitigation potential of the MREs in this study.

$$CPP(x,y)[years] = \frac{GW_{MRE\ array}(x,y)[gCo2eq./kWh]}{GW_{Ref} - GW_{MRE}[gCo2eq./kWh]} \cdot L[years] \quad (12)$$

3. Results

3.1. Impact maps

For the studied MRE arrays, the geospatial distribution of climate change mitigation potential is shown in Fig. 8 in terms of GW impacts and CPP. In the first column, GW impacts with an upper limit of 1000 $gCO_2eq./kWh$, corresponding to the impact level of electricity from a coal power plant [49], are shown. Areas with low GW impacts under 100 $gCO_2eq./kWh$ which mark potential deployment locations where MREs can be operated with impact levels contributing to climate change mitigation, are presented in the middle column. The right column shows the corresponding CPPs. Carbon payback must be realised within the lifetime of the device to be considered carbon-neutral, and for it to be able to contribute positively to climate change mitigation. Therefore, only areas with CPPs lower than 20 years relative to the carbon intensity of the 2022 average European electricity mix are presented. The maps contain only those parts of each technology's water-depth-restricted theoretically applicable area (see Fig. 5) that fulfil the aforementioned conditions.

The distribution of impacts across the area shows a similar pattern to the CFs of the MREs (see Fig. 5), suggesting a large influence of the CF on the overall impact per kWh of electricity produced at a location.

For the FPV, a decrease in impact with increasing CFs at lower latitudes can be observed, with a minimum of 385 $gCO_2eq./kWh$ being achieved in southern France, and at the Portuguese west coast close to shore where the water is still relatively shallow (up to 40 m). The FPV doesn't reach impact levels below the carbon intensity of the current European electricity mix which is used as a reference for the CPP. This means the FPV plant in the studied area is not able to pay back its life cycle carbon emissions within a European electricity grid, regardless of its lifetime. Therefore such plot is not shown.

For the two different types of WECs, a large difference in performance can be observed. PAs reach carbon payback during their lifetime in 73 % of the theoretically applicable area, while for the OWSC these areas are scarce with 2 %, limited to some bays close to shore of the Irish and Scottish west coasts. Here, minimum impacts of 78 $gCO_2eq./kWh$ can be achieved. Due to the widespread occurrence of low CFs, the average impacts are significantly higher at 543 $gCO_2eq./kWh$ and carbon payback cannot be achieved in most areas, similar to the FPV. This limits the potential applications of the OWSC WEC to niche applications in European coastal waters, highlighting advantages of the more versatile PA for large-scale applications over the OWSC. For the PAs, carbon-neutral deployment areas are spread along the coastlines that are not shaded from waves by landmasses, like the Western Isles, the coast of Galicia, Spain and Brittany, France as well as the west coast of Ireland. Here, minimum impacts of 50 $gCO_2eq./kWh$ are achieved. Due to much higher impacts, shaded areas like the English Channel, the east coast of Great Britain (GB), the Irish Sea, and areas between islands around Scotland are eliminated as feasible deployment locations for carbon-neutral deployment.

The impacts of the FOWT show lower variations across the studied area with a slight increase at higher latitudes. Impacts as low as 17 $gCO_2eq./kWh$ are achieved in areas spread around GB and Ireland, where sufficient water depth is reached relatively close to shore. FOWTs achieve impacts sufficiently low for carbon-neutral deployment across nearly the near-full applicable area (99 %) with little exceptions in slightly shaded, deep water areas on the north coast of Spain, where impacts reach up to 181 $gCO_2eq./kWh$.

Large parts of the the North Sea are unfeasible for marine renewable deployment with climate change mitigation benefits, due to too low water depth (FOWT and PA) or insufficient wave energy flux and solar irradiation (WEC and FPV).

A summary of key parameters of the results is given in Table 3.

Although a high CF is the strongest driver of low global warming impacts, minimal impact value is not always achieved at the point with the highest CF, but tends to be located closer to shore because of the influences of cable length to shore and mooring intensity according to water depth.

3.2. Contribution analysis

To directly compare and study the major drivers of GW impacts within the four technologies, a component-based contribution analysis for the MREs' standard conditions (average CF, water depth and distance to shore) in their applicable deployment area is performed. The comparison is shown in Fig. 9.

The FPV's global warming impacts per produced unit of electricity are significantly larger than those of the other MREs. Striking is the higher share of impacts coming from vessel operations for the FPV. This is due to the considered mooring system with six lines and the assumptions on the vessel activities related to catenary moorings, taking separate installation and connection times for each chain into account when installing, disconnecting, and reconnecting for corrective maintenance. The share of impacts from the power generator varies between technologies, being lowest for the PA linear generator and highest for

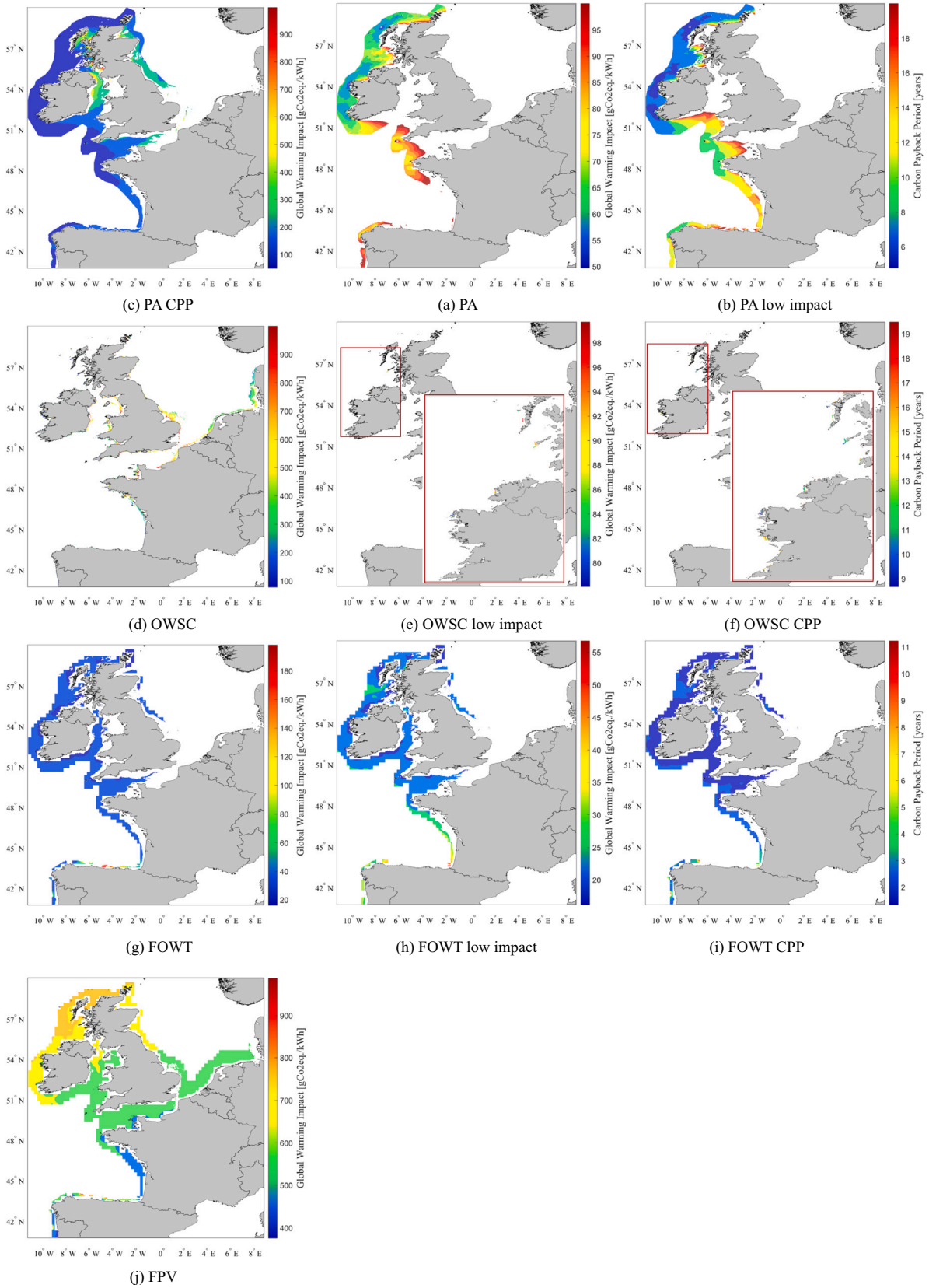

Fig. 8. Spatial distribution of the global warming impacts and associated carbon payback periods from different MRE arrays, including export cables and moorings.

Table 3
Summary of environmental performance parameters of MRE arrays including the lowest achievable CPPs and GW impacts in the applicable areas, corresponding deployment locations and their characteristics as well as statistical indicators.

	PA	OWSC	FPV	FOWT
Min. GW [gCo2eq/kWh]	50	78	385	17
Min. CPP [yr]	4,7	8,7	Na	1,4
Location	Ireland, west of Keem	Ireland, east of Inishkea Island	Portugal, south of Porto	Orkney Islands
Dist. at min [km]	18	25	25	8
Depth at min [m]	50	19	29	75
CF at min [%]	33	39	15	56
Max. CF [%]	36	39	15	61
Avg. GW [gCo2eq/kWh]	126	543	590	24
Avg. CF [%]	20	8	10	51
Carbon-neutral area[2] [%]	72	3	0	99
Array size	33	20	40	2

[2] With respect to each technology's theoretically applicable area in terms of water depth, as shown in Fig. 5.

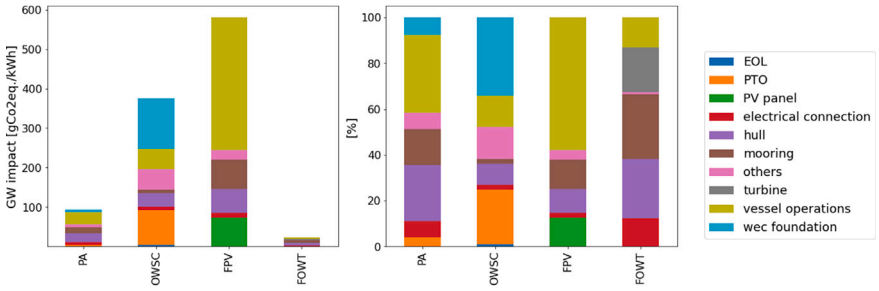

Fig. 9. Absolute and relative comparison of global warming impacts and component contributions of the average studied MRE arrays.

the OWSC hydraulic PTO. In absolute terms, impacts per kWh of the hydraulic PTO and the PV panels exceed the total impact of the FOWT. The OWSC's large reinforced concrete foundation leads to a higher share of the foundation compared to the PA. Most global warming impacts stem from used materials within the components, and secondly from offshore vessel operations. Material processing and transport only make up around 10 % (not shown in Fig. 9 as included in the components) [44].

3.3. Influence of array size and periphery

As shown in Fig. 9, impact shares of the export cable are low for all MRE arrays. This is contradictory to the results found in Engelfried et al. [44], where the cable contributed nearly 60 % to the GW impacts of a single WEC. To understand the influences of array size in relation to the periphery, the climate change impact for a single device connected to the grid with an export cable is assessed (Fig. 10) and compared to the absolute results and component contributions obtained for the grid-connected array and a non-grid connected device without cable (standalone) (Fig. 11).

The impact map of the single grid-connected PA (Fig. 10) shows a significantly different pattern than the one for the array scaled to the capacity of the electrical cable (25 MW - 33 PAs) (Fig. 8). The patterns of the distribution of the distance to shore (see Fig. 3) are much more prominent, showing increasing impact with distance to shore, regardless of the CF. The reason for the increased relevance of the distance to shore in the impact distribution of a single device is the high share of impacts per kWh, that can be attributed to the material-intensive electrical cable, which increases in length with distance to shore. As shown in Fig. 11, 67 % of GW impacts per kWh electricity from the single grid connected PA stem from the electrical cable. This is nearly ten times higher than for the PA array (Fig. 9). Furthermore, the single connected PA has significantly larger overall GW impacts per kWh (339 $gCO_2eq./kWh$) than for the array (92 $gCO_2eq./kWh$). This shows that arraying increases the utilization of the cable, holding significant potential for reducing MREs impacts per kWh.

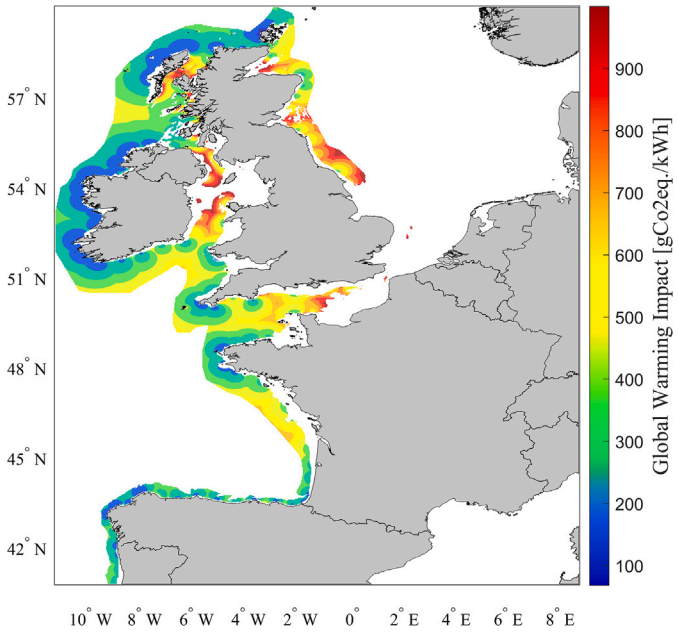

Fig. 10. Spatial distribution of global warming impacts from a single PA connected to the grid with an export cable.

A standalone PA without cable presents impacts of 94 $gCO_2eq./kWh$, higher than those for the array. The additional reduction of impacts in an array, to levels below the standalone device, is achieved by sharing the transit of the inspection vessels for maintenance.

4. Discussion

The geospatial distribution of global warming impacts from different MREs presented in this study shows great variability across the European

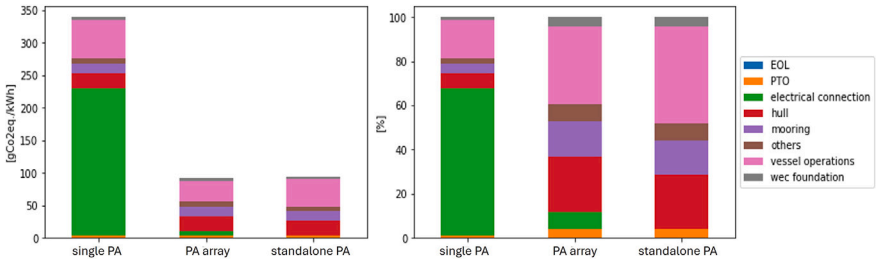

Fig. 11. Absolute and relative comparison of global warming impacts and component contributions of a single grid-connected PA (incl. cable), a PA array (incl. cable) and a standalone PA (no cable) under standard conditions.

Atlantic coastlines and the North Sea. Not everywhere where an MRE can be theoretically deployed, can carbon neutrality be achieved. This highlights a strong importance of the site for sustainable MRE deployment with a positive contribution to climate change mitigation. Implications of these findings, drivers of variations, as well as the study's limitations are discussed in the following sections.

4.1. Effects of MRE arraying

For all studied MRE arrays, the most important factor for low-impact deployment is the CF and the resulting electricity production at a location. Water depth influences are minor and are more relevant for the impact distribution for mooring-intensive devices such as the FOWT and FPV or others not presented in this study, which also make use of catenary moorings. The importance of the distance to shore, which drives the length of the export cable, varies with array size. For single grid-connected devices, impacts are dominated by the distance to shore, which drives impacts of the electrical cable. With increasing installed power relative to the cable capacity, the most influential location factor for low environmental impacts shifts from short distance to shore to a high CF. Overall impacts per kWh are reduced for arrays with maximal cable utilization, and impact levels lower than those of a standalone device are achieved. This confirms that infrastructure and maintenance sharing between devices in arrays is beneficial for reducing environmental impacts of MREs, as highlighted by Engelfried et al. [44]. Similarly, it can be expected that shared mooring systems in an array will lead to significant impact reductions. Future research should explore the potential changes in environmental impacts of hybrid arrays combining different MRE technologies. In addition, to opportunities for shared infrastructure and maintenance, such arrays may influence overall power production patterns through complementary intermittency profiles and integration with storage options, with potential positive wider implications for the European electricity grid.

This study does not consider hydrodynamic interactions between WECs in an array, as sufficient spacing between the devices is assumed. However, for real-world scenarios, these effects can significantly affect the overall power output depending on array layout, incident wave direction, device geometry and spacing [97]. Certain array configurations could lead to an increase in power output of up to 20 % while others could lead to a reduction of up to 20 % and potentially more due to destructive interactions [63,97,119,120]. Changes in electricity production linearly increase or decrease environmental impact of the MRE per kWh. Positive hydrodynamic interactions within a large array would therefore lead to potentially even higher impact reductions compared to a single device. For the case of negative interactions, trade-offs with reductions in impacts through shared infrastructure need to be evaluated for every case. Based on this representative analysis, which reveals a 70 % reduction of GW impacts from a single device to an optimally sized array (see Section 3.3), the significant reduction of periphery impacts is expected to outweigh potential negative array interactions from an environmental perspective.

4.2. Material influences

The contribution analysis showed that the majority of impacts stem from the materials the MRE is built of, largely steel and other metals. A major driver of differences between the performance of the technologies is their ratio of material to energy production determined by RP and CF. Table 4 shows these ratios for the studied devices.

Both PA and FOWTs have been shown to be able to reach carbon neutrality in widespread areas, where sufficient electricity output at suitable locations in terms of water depth and distance to shore can be achieved. Both technologies show relatively low weight to lifetime produced energy ratios. FOWTs are the overall heaviest structures with the large semi-submersible platform, turbine and heavy mooring, yet this is compensated by a large RP and good average CF, making their impacts the overall lowest, and carbon-neutrality reachable already within 1.4 years. The PA has a lower RP compared to the FOWT, making low impacts more dependent on the CF. Higher impact variations across the area are therefore observed and carbon neutrality is only reached where a suitable wave resource can be found.

The OWSC has the highest weight to RP ratio, followed by the FPV and on average low CFs lead to high lifetime energy output to weight ratios. Both devices show high impacts across the study area. The OWSC is large in size and has a material-intensive PTO, yet with twice the RP of the FPV and higher best-case CFs, it can achieve sufficiently low impacts to reach carbon neutrality in 9 years in a few locations with optimal wave conditions. The pontoon-type FPV plant, in contrast, cannot be considered a carbon-neutral technology within the totality of the studied area. Minimum achieved impact levels are not lower than those of the current European electricity mix. FPV plants for deployment in these areas require large and material-intensive structures for survivability in harsh wave climates, while CFs achievable with the solar irradiation in the northern hemisphere far from the Equator are not sufficient with current PV technology. This combination results in the high material to produced energy ratio. An increased density of PV panel surface on the structure or a less material-intensive structure such as flexible superficial FPVs could potentially decrease the technology's environmental impact. However, these are less developed, whilst survivability in rough North Sea and North Atlantic climates as well as economic competitiveness is still unclear [121].

Apart from decreasing the material intensity of the produced electricity, a change in floater material from steel to low-impact fibre-reinforced

Table 4
Comparison of the weight (mooring, foundation and floater) to rated power and lifetime electricity production ratio of the different modelled MREs - based on the average CF in the applicable area.

	PA	OWSC	FPV	FOWT
Weight [t]	396	1163	561	5063
RP ratio [kg/kW]	660	1163	1122	533
LEP ratio [g/kWh]	19	83	64	6

concrete could further reduce the environmental impact of MRE devices. As shown by Engelfried et al. [44], the alternative material [122] nearly eliminates GW impacts of the floater hull. Based on the contribution analysis in Section 3.2, this highlights a particularly prominent improvement potential for the PA and FOWT, of around 30 %. For the OWSC and FPV, a lower reduction potential of ~10 % is expected as their impacts are dominated by other factors such as the hydraulic PTO and vessel operations.

In addition, to being concentrated in the structural materials, GW impacts are largely associated with the manufacturing and assembly phases of MREs. Impacts from the disposal and end-of-life phase are negligible, as demonstrated in a prior study [44] and by Garcia-Teruel et al. [58]. For technologies with uncertain recycling pathways, such as PV cells and GFRP blades of FOWTs, worst-case assumptions were applied, considering incineration or landfilling under different national standards and without further recycling efforts. Potential reductions in impacts through advanced recycling techniques—such as co-processing in cement production or material separation in PV cells—are therefore not anticipated to significantly affect the results, particularly regarding global warming impacts and carbon payback times.

4.3. Limitations

The impact maps obtained in this study should serve as an indication of potentially feasible areas of deployment for MREs in European waters, and are not meant to represent absolute impacts of specific projects at specific locations due to limitations in fidelity of assumptions. The results should encourage the thorough assessment of local environmental impacts at possible deployment locations before project execution. Only this will enable the actual contribution of MRE installations to climate change mitigation.

Limitations in the accuracy of results are imposed by a low level of fidelity in assumptions in parts of the underlying LCIs and spatial data. For offshore activities and maintenance regimes differences in procedures and failure rates of parts are not taken into account. Engelfried et al. [44], performed a sensitivity analysis on different maintenance regimes for a PA WEC, and revealed that the frequency of tow backs significantly influenced GW impacts, increasing them by more than double when the tow-back frequency was increased to annual. The combination of the already underlying uncertainty in industry practices in that field, and their high importance for impact results [44,52,58], marks a hotspot that should be further investigated, especially for other MREs besides offshore wind. Furthermore, limiting the requirement for extensive corrective maintenance is therefore an important factor in supporting the environmental sustainability of MREs.

Furthermore, as mentioned above, limitations are imposed by disregarding a specific array layout and system configuration (inter-array cables, device interactions, transmission losses), as well as spatially explicit supply ports and respective travel distances for offshore vessels. Disregarding transmission losses in the export cable can lead to an underestimation of the overall impact per kWh, which is proportional to the magnitude of the losses as they directly affect the plant's overall power output. For the chosen grid connection, this equates to around 6 %, increasing with distances to shore greater than 70 km [123]. This is expected to be consistent across all assessed technologies, introducing no changes in the comparison of MREs.

Assuming constant port distances of 100 km reduces uncertainty in choosing possible port routings that depend on various factors besides the distance between the plant and the port. Due to the first-of-its-kind large area included in the study, different port options for every data point are considered to be out of scope. The 100 km distance is considered representative of most theoretical deployment locations due to the large density of (especially smaller) supply ports along the coasts of the studied area. A previous study has performed a sensitivity analysis on the distance to port which showed a 5 % increase in impacts for 10 % increase in port distance [44]. This suggests that selecting ports located more than 200 km away can substantially amplify the environmental impact of MRE projects. Therefore, the distance to port is a critical parameter in port selection, as it directly affects the overall environmental feasibility of an MRE plant.

The underlying spatial data for wind speeds, solar irradiation, and temperature from ERA5 have lower temporal coverage and resolution than the WEC data that were available within the working group for this study, limiting direct comparability. Overall conclusions from the results are not affected by these limitations, however, direct comparison between the MREs at specific locations should not be inferred.

5. Conclusion

In this study, a first-of-its-kind geospatial analysis of life cycle global warming impacts from four different MRE technologies within an area of growing interest, the North Sea and North Atlantic European waters is presented. The study combines a detailed representative LCA model of two WEC types, FPV, and FOWT with spatial resource and bathymetry data, to obtain impact maps for the studied devices. The distribution of global warming impacts and associated carbon payback periods across the studied area was assessed, and potential low-impact areas, as well as the major contributors within the devices were identified. The study results enable incorporating climate change mitigation potential of MREs into decision making and site selection for MREs in a phase of growing importance for EU energy transition targets.

It is found that not all MREs are equally suitable for a potential large-scale contribution to climate change mitigation in Europe. Global warming impacts vary strongly across the technologies and between sites. The OWSC WEC can reach a minimum global warming impact of 78 $gCO_2eq./kWh$ with a corresponding carbon payback period of 8.6 years. However, this is limited to very few locations on the west coast of Ireland, with the majority of sites being not feasible for carbon-neutral deployment due to impact levels not being low enough for carbon payback in the European electricity grid within the plant's lifetime. FPVs do not achieve carbon neutrality at any location in the studied area, with a minimum impact of 385 $gCO_2eq./kWh$, which is more than 100 g higher than the current average carbon intensity of the European electricity mix. From a life cycle environmental perspective, rigid pontoon-type FPVs can therefore not be considered a beneficial renewable energy technology for contributing to climate change mitigation, when deployed in European waters. This is due to their material-intensive structure and low power output.

For the FOWT and PA, overall low impact levels and carbon payback periods are found, suggesting them as good potential candidates for large-scale MRE deployment in European waters. The PA achieves carbon-neutral impact levels in 73 % of the theoretically applicable area, with a minimum global warming impact of 50 $gCO_2eq./kWh$ and a corresponding carbon payback period of 4.7 years. Best potential sites are spread along the North Atlantic coast. FOWTs achieve sufficiently low impact levels across the near-full theoretically applicable area, with a minimum impact of 17 $gCO_2eq./kWh$, leading to lowest carbon payback periods of 1.4 years. This makes FOWTs competitive with the further developed BOWTs from an environmental perspective.

For all MRE arrays, high capacity factors were found to be the most influential location parameter for achieving low impact levels. For single grid-connected devices or arrays not scaled to the transmission infrastructure, distance to shore is more important and impacts per kWh are much higher due to the carbon intensity of the cabling. These findings highlight the need to share infrastructure such as the transmission cable and, in the future, possibly moorings by deploying MREs in arrays. Like this, infrastructure utilization is maximised and its contribution to the overall impact per kWh is reduced.

The findings highlight the critical importance of assessing the site-specific environmental performance of MRE projects and integrating

these outcomes into decision making processes to ensure their effective contribution to a carbon-neutral energy future.

CRediT authorship contribution statement

Tabea Engelfried: Conceptualization, data curation, formal analysis, investigation, methodology, visualization, writing - original draft. **Matias Alday:** Data curation, formal analysis. **Vaibhav Raghavan:** Data curation, formal analysis, writing - review & editing. **George Lavidas:** Conceptualization, visualization, funding acquisition, project administration, supervision, writing - review & editing

Declaration of competing interest

The authors declare that they have no known competing financial interests or personal relationships that could have appeared to influence the work reported in this paper.

Acknowledgements

This research was funded by the Dutch Research Council (Nederlandse Organisatie voor Wetenschappelijk Onderzoek-NWO) (EP.1602.22.001) and the CETPartnership, the Clean Energy Transition Partnership under the 2022 CETPartnership joint call for research proposals, co-funded by the European Commission (GAN°101069750) Project No. CETP-2022–00127.

Appendix A. Supplementary material

The following document contains the life cycle inventory data for the presented model including a a list of parameters, used data points, sources and assumptions.

Appendix B. Supplementary data

Supplementary data for this article can be found online at doi:10.1016/j.rser.2025.116338.

Data availability

Data that is not already available open-access is shared as supplementary material.

References

[1] Lee H, Romero J. Climate change 2023: Synthesis report. Contribution of working groups I, II and III to the sixth assessment report of the Intergovernmental Panel on Climate Change., Tech. rep., Geneva, Switzerland: IPCC; 2023. https://doi.org/10.59327/IPCC/AR6-9789291691647
[2] Paris agreement. 2016. https://eur-lex.europa.eu/legal-content/EN/TXT/?uri=CELEX:22016A1019(01)
[3] IEA. Renewables 2023, Tech. rep., Paris (2024). https://www.iea.org/reports/renewables-2023
[4] Chen L, Msigwa G, Yang M, Osman AI, Fawzy S, Rooney DW, et al. Strategies to achieve a carbon neutral society: a review. Environ Chem Lett 2022;20(4):2277–310. https://doi.org/10.1007/s10311-022-01435-8
[5] Gielen D, Boshell F, Saygin D, Bazilian MD, Wagner N, Gorini R. The role of renewable energy in the global energy transformation. Energy Strateg Rev 2019;24:38–50. https://doi.org/10.1016/j.esr.2019.01.006
[6] McKenna R, Mulalic I, Soutar I, Weinand JM, Price J, Petrović S, et al. Exploring trade-offs between landscape impact, land use and resource quality for onshore variable renewable energy: an application to Great Britain. Energy 2022;250:123754. https://doi.org/10.1016/j.energy.2022.123754
[7] Tröndle T. Supply-side options to reduce land requirements of fully renewable electricity in Europe. PLoS One 2020;15(8):e0236958. https://doi.org/10.1371/journal.pone.0236958
[8] Turney D, Fthenakis V. Environmental impacts from the installation and operation of large-scale solar power plants. Renew Sustain Energy Rev 2011;15(6):3261–70. https://doi.org/10.1016/j.rser.2011.04.023
[9] European Commission. Communication from the commission to the European parliament, the council, the European economic and social committee and the committee of the regions an EU strategy to harness the potential of offshore renewable energy for a climate neutral future (COM(2020) 741). 2020. https://eur-lex.europa.eu/legal-content/EN/TXT/?uri=COM:2020:741:FIN
[10] Wind Europe. Latest wind energy data for Europe - autumn 2024, Tech. rep. (2024 Sep) https://windeurope.org/intelligence-platform/product/latest-wind-energy-data-for-europe-autumn-2024/?utm_source=chatgpt.com
[11] Equinor ASA. Hywind Tampen. https://www.equinor.com/energy/hywind-tampen
[12] Equinor ASA. Hywind Scotland. https://www.equinor.com/energy/hywind-scotland
[13] Principle Power. Projects. https://www.principlepower.com/projects
[14] SolarDuck. Solarduck and RWE successfully install offshore floating solarpilot Merganser off Dutch coast. 2024 Jul https://solarduck.tech/solarduck-and-rwe-successfully-install-offshore-floating-solar-pilot-merganser-off-dutch-coast/
[15] Oceans of Energy. North Sea 2 - 1MW. https://oceansofenergy.blue/north-sea-2/
[16] Satymov R, Bogdanov D, Dadashi M, Lavidas G, Breyer C. Techno-economic assessment of global and regional wave energy resource potentials and profiles in hourly resolution. Appl Energy 2024;364:123119. https://doi.org/10.1016/J.APENERGY.2024.123119
[17] Lavidas G, Blok K. Shifting wave energy perceptions: the case for wave energy converter (WEC) feasibility at milder resources. Renew Energy 2021;170:1143–55. https://doi.org/10.1016/j.renene.2021.02.041. https://linkinghub.elsevier.com/retrieve/pii/S0960148121002093
[18] Reikard G. Integrating wave energy into the power grid: simulation and forecasting. Ocean Eng 2013;73:168–78. https://doi.org/10.1016/j.oceaneng.2013.08.005. https://www.sciencedirect.com/science/article/pii/S0029801813003399
[19] Kluger JM, Haji MN, Slocum AH. The power balancing benefits of wave energy converters in offshore wind-wave farms with energy storage. Appl Energy 2023;331:120389. https://doi.org/10.1016/j.apenergy.2022.120389. https://www.sciencedirect.com/science/article/pii/S0306261922016464
[20] Weiss CVC, Guanche R, Ondiviela B, Castellanos OF, Juanes J. Marine renewable energy potential: a global perspective for offshore wind and wave exploitation. Energy Convers Manag 2018;177:43–54. https://doi.org/10.1016/j.enconman.2018.09.059. https://linkinghub.elsevier.com/retrieve/pii/S0196890418310628
[21] Tsai L, Kelly JC, Simon BS, Chalat RM, Keoleian GA. Life cycle assessment of offshore wind farm siting: effects of locational factors, lake depth, and distance from shore. J Ind Ecol 2016;20(6):1370–83. https://doi.org/10.1111/jiec.12400
[22] Blanc I, Guermont C, Gschwind B, Ménard L, Calkoen C, Zelle H. Web tool for energy policy decision-making through geo-localized LCA models: a focus on offshore wind farms in Northern Europe. In: EnviroInfo 2012 - 26th international conference on informatics for environmental protection; Dessau, Germany: 2012. p. 499–506.
[23] Portilla J, Sosa J, Cavaleri L. Wave energy resources: Wave climate and exploitation. Renew Energy 2013;57:594–605. https://doi.org/10.1016/j.renene.2013.02.032
[24] Guo B, Ringwood JV. A review of wave energy technology from a research and commercial perspective. IET Renew Power Gener 2021;15(14):3065–90. https://doi.org/10.1049/rpg2.12302. https://onlinelibrary.wiley.com/doi/abs/10.1049/rpg2.12302
[25] Martinez A, Iglesias G. Mapping of the levelised cost of energy for floating offshore wind in the European Atlantic. Renew Sustain Energy Rev 2022;154:111889. https://doi.org/10.1016/j.rser.2021.111889
[26] Martinez A, Iglesias G. Mapping of the levelised cost of energy from floating solar PV in coastal waters of the European Atlantic, North Sea and Baltic Sea. Solar Energy 2024;279:112809. https://doi.org/10.1016/j.solener.2024.112809. https://linkinghub.elsevier.com/retrieve/pii/S0038092X24005048
[27] O'Connell R, Kamidelivand M, Furlong R, Guerrini M, Cullinane M, Murphy J. An advanced geospatial assessment of the levelised cost of energy (LCOE) for wave farms in Irish and western UK waters. Renew Energy 2024;221:119864. https://doi.org/10.1016/j.renene.2023.119864. https://linkinghub.elsevier.com/retrieve/pii/S0960148123017792
[28] Gunn K, Stock-Williams C. Quantifying the global wave power resource. Renew Energy 2012;44:296–304. https://doi.org/10.1016/J.RENENE.2012.01.101
[29] Guillou N, Lavidas G, Chapalain G. Wave energy resource assessment for exploitation–a review. J Mar Sci Eng 2020;8(9):705. https://doi.org/10.3390/jmse8090705. https://www.mdpi.com/2077-1312/8/9/705
[30] Soares PMM, Lima DCA, Nogueira M. Global offshore wind energy resources using the new ERA-5 reanalysis. Environ Res Lett 2020;15(10):1040a2. https://doi.org/10.1088/1748-9326/abb10d
[31] Zheng CW, Li CY, Pan J, Liu MY, Xia LL. An overview of global ocean wind energy resource evaluations. Renew Sustain Energy Rev 2016;53:1240–51. https://doi.org/10.1016/j.rser.2015.09.063
[32] Silalahi DF, Blakers A. Global atlas of marine floating solar PV potential. Solar 2023;3(3):416–33. https://doi.org/10.3390/solar3030023. https://www.mdpi.com/2673-9941/3/3/23
[33] Guillou N, Lavidas G, Kamranzad B. Wave energy in Brittany (France)–resource assessment and – performances. Sustainability 2023;15(2):1725. https://doi.org/10.3390/su15021725
[34] DeCastro M, Lavidas G, Arguilé- Pérez B, Carracedo P, DeCastro NG, Costoya X, et al. Evaluating the economic viability of near-future wave energy development along the Galician coast using LCoE analysis for multiple wave energy devices. J Clean Prod 2024;463:142740. https://doi.org/10.1016/j.jclepro.2024.142740
[35] Caglayan DG, Ryberg DS, Heinrichs H, Linßen J, Stolten D, Robinius M. The techno-economic potential of offshore wind energy with optimized future turbine designs in Europe. Appl Energy 2019;255:113794. https://doi.org/10.1016/j.apenergy.2019.113794
[36] Lavidas G. Selection index for wave energy deployments (SIWED): a near-deterministic index for wave energy converters. Energy 2020;196:117131. https://doi.org/10.1016/j.energy.2020.117131

[37] Maldonado AD, Galparsoro I, Mandiola G, de Santiago I, Garnier R, Pouso S, et al. A Bayesian network model to identify suitable areas for offshore wave energy farms, in the framework of ecosystem approach to marine spatial planning. Sci Total Environ 2022;838:156037. https://doi.org/10.1016/j.scitotenv.2022.156037

[38] Hammar L, Gullström M, Dahlgren TG, Asplund ME, Goncalves IB, Molander S. Introducing ocean energy industries to a busy marine environment. Renew Sustain Energy Rev 2017;74:178–85. https://doi.org/10.1016/j.rser.2017.01.092. https://www.sciencedirect.com/science/article/pii/S1364032117301090

[39] Bao M, Arzaghi E, Abaei MM, Abbassi R, Garaniya V, Abdussamie N, et al. Site selection for offshore renewable energy platforms: a multi-criteria decision-making approach. Renew Energy 2024;229:120768. https://doi.org/10.1016/j.renene.2024.120768

[40] Kamranzad B, Hadadpour S. A multi-criteria approach for selection of wave energy converter/location. Energy 2020;204:117924. https://doi.org/10.1016/j.energy.2020.117924

[41] Choupin O, Pinheiro Andutta F, Etemad-Shahidi A, Tomlinson R. A decision-making process for wave energy converter and location pairing. Renew Sustain Energy Rev 2021;147:111225. https://doi.org/10.1016/j.rser.2021.111225

[42] Guinée JB. Handbook on life cycle assessment. 2002;7. https://doi.org/10.1007/0-306-48055-7. http://link.springer.com/10.1007/0-306-48055-7

[43] Paredes MG, Padilla-Rivera A, Güereca LP. Life cycle assessment of ocean energy technologies: a systematic review. J Mar Sci Eng 2019;7(9):322. https://doi.org/10.3390/jmse7090322. https://www.mdpi.com/2077-1312/7/9/322

[44] Engelfried T, Cucurachi S, Lavidas G. Life cycle assessment of a point absorber wave energy converter. Clean Environ Syst 2025:100265. https://doi.org/10.1016/j.cesys.2025.100265. https://linkinghub.elsevier.com/retrieve/pii/S266678942500011X

[45] Thomson RC, Chick JP, Harrison GP. An LCA of the Pelamis wave energy converter. Int J Life Cycle Assess 2019;24(1):51–63. https://doi.org/10.1007/s11367-018-1504-2

[46] Pennock S, Vanegas-Cantarero MM, Bloise-Thomaz T, Jeffrey H, Dickson MJ. Life cycle assessment of a point-absorber wave energy array. Renew Energy 2022;190:1078–88. https://doi.org/10.1016/j.renene.2022.04.010. https://linkinghub.elsevier.com/retrieve/pii/S0960148122004712

[47] Apolonia M, Simas T. Life cycle assessment of an oscillating wave surge energy converter. J Mar Sci Eng 2021;9(2):206. https://doi.org/10.3390/jmse9020206. https://www.mdpi.com/2077-1312/9/2/206

[48] Arvesen A, Hertwich EG. Assessing the life cycle environmental impacts of wind power: a review of present knowledge and research needs. Renew Sustain Energy Rev 2012;16(8):5994–6006. https://doi.org/10.1016/j.rser.2012.06.023

[49] United Nations Economic Commission for Europe. Carbon neutrality in the UNECE region: integrated life-cycle assessment of electricity sources, Tech. rep. (2022). https://unece.org/sed/documents/2021/10/reports/life-cycle-assessment-electricity-generation-options

[50] Turconi R, Boldrin A, Astrup T. Life cycle assessment (LCA) of electricity generation technologies: overview, comparability and limitations. Renew Sustain Energy Rev 2013;28:555–65. https://doi.org/10.1016/j.rser.2013.08.013. https://linkinghub.elsevier.com/retrieve/pii/S1364032113005534

[51] Kaldellis JK, Apostolou D. Life cycle energy and carbon footprint of offshore wind energy. Comparison with onshore counterpart. Renew Energy 2017;108:72–84. https://doi.org/10.1016/j.renene.2017.02.039

[52] Arvesen A, Birkeland C, Hertwich EG. The importance of ships and spare parts in LCAs of offshore wind power. Environ Sci Technol 2013;47(6):2948–56. https://doi.org/10.1021/es304509r. https://pubs.acs.org/doi/10.1021/es304509r

[53] Weinzettel J, Reenaas M, Solli C, Hertwich EG. Life cycle assessment of a floating offshore wind turbine. Renew Energy 2009;34(3):742–7. https://doi.org/10.1016/j.renene.2008.04.004

[54] Poujol B, Prieur-Vernat A, Dubranna J, Besseau R, Blanc I, Pérez-López P. Site-specific life cycle assessment of a pilot floating offshore wind farm based on suppliers' data and geo-located wind data. J Ind Ecol 2020;24(1):248–62. https://doi.org/10.1111/jiec.12989

[55] Yildiz N, Hemida H, Baniotopoulos C. Life cycle assessment of a barge-type floating wind turbine and comparison with other types of wind turbines. Energies 2021;14(18):5656. https://doi.org/10.3390/en14185656

[56] Brussa G, Grosso M, Rigamonti L. Life cycle assessment of a floating offshore wind farm in Italy. Sustain Prod Consum 2023;39:134–44. https://doi.org/10.1016/j.spc.2023.05.006. https://www.sciencedirect.com/science/article/pii/S235255092300101X

[57] Struthers IA, Avanessova N, Gray A, Noonan M, Thomson RC, Harrison GP. Life cycle assessment of four floating wind farms around Scotland using a site-specific operation and maintenance model with SOVs. Energies 2023;16(23):7739. https://doi.org/10.3390/en16237739

[58] Garcia-Teruel A, Rinaldi G, Thies PR, Johanning L, Jeffrey H. Life cycle assessment of floating offshore wind farms: an evaluation of operation and maintenance. Appl Energy 2022;307:118067. https://doi.org/10.1016/J.APENERGY.2021.118067

[59] Cromratie Clemons SK, Salloum CR, Herdegen KG, Kamens RM, Gheewala SH. Life cycle assessment of a floating photovoltaic system and feasibility for application in Thailand. Renew Energy 2021;168:448–62. https://doi.org/10.1016/j.renene.2020.12.082. https://linkinghub.elsevier.com/retrieve/pii/S096014812032022X

[60] Pulselli RM, Maccanti M, Bruno M, Sabbetta A, Neri E, Patrizi N, et al. Benchmarking marine energy technologies through LCA: offshore floating wind farms in the Mediterranean. Front Energy Res 2022 Jun;10. https://doi.org/10.3389/fenrg.2022.902021

[61] Final report summary - ENERGEO (Earth observation for monitoring and assessment of the environmental impact of energy use). 2013. https://cordis.europa.eu/project/id/226364/reporting

[62] Mendecka B, Lombardi L. Life cycle environmental impacts of wind energy technologies: a review of simplified models and harmonization of the results. Renew Sustain Energy Rev 2019;111:462–80. https://doi.org/10.1016/j.rser.2019.05.019

[63] Raghavan V, Alday G. M, Metrikine A, Lavidas G. Wave energy farm assessment in real wave climates: The North Sea. 2024 Aug https://doi.org/10.1115/OMAE2024-120946. https://dx.doi.org/10.1115/OMAE2024-120946

[64] CorPower Ocean. Corpower ocean - projects. 2024. https://corpowerocean.com/projects/

[65] CorPower Ocean. Corpower ocean completing C4 inspection and upgrades. 2024 Jul https://corpowerocean.com/corpower-ocean-completing-inspection-upgrades/

[66] CorPower Ocean. First commercial scale UMACK anchor deployed offshore, Portugal. 2022. https://corpowerocean.com/corpower-ocean-first-anchor-deployed/

[67] Karan H, Thomson RC, Harrison GP. Full life cycle assessment of two surge wave energy converters. Proc Inst Mech Eng Part A J Power Energy 2020;234(4):548–61. https://doi.org/10.1177/0957650919867191

[68] Apolonia M. Developing the PTO of the first MW-level oscillating wave surge converter collaborative project - D5.3 final LCA report of the MegaRoller device, Tech. rep. (2020). https://zenodo.org/records/5749475

[69] Cerveira F, Fonseca N, Pascoal R. Mooring system influence on the efficiency of wave energy converters. Int J Mar Energy 2013;3-4:65–81. https://doi.org/10.1016/j.ijome.2013.11.006. https://www.sciencedirect.com/science/article/pii/S2214166913000325

[70] Depalo F, Wang S, Xu S, Guedes Soares C. Design and analysis of a mooring system for a wave energy converter. J Mar Sci Eng 2021;9(7):782. https://doi.org/10.3390/jmse9070782. https://www.mdpi.com/2077-1312/9/7/782

[71] SolarDuck. Merganser pilot. 2024. https://solarduck.tech/merganser-pilot/

[72] Pecher A, Foglia A, Kofoed JP. Comparison and sensitivity investigations of a CALM and SALM type mooring system for wave energy converters. J Mar Sci Eng 2014;2(1):93–122. https://doi.org/10.3390/jmse2010093. https://www.mdpi.com/2077-1312/2/1/93

[73] Harris R, Johanning L, Wolfram J. Mooring systems for wave energy converters: a review of design issues and choices. Proc Inst Mech Eng Part B J Eng Manuf 2006;220:159–68.

[74] Allen C, Viselli A, Dagher Andrew Goupee H, Gaertner E, Abbas N, Hall M, et al. Definition of the UMaine VolturnUS-S reference platform developed for the IEA wind 15-megawatt offshore reference wind turbine technical report, Tech. rep. (2020). www.nrel.gov/publications

[75] ATKINS. Kincardine offshore windfarm - environmental statement. 2016. https://marine.gov.scot/data/kincardine-offshore-windfarm-environmental-statement-and-appendices

[76] Statoil. Hywind Scotland pilot park - Environmental statement. 2015. https://marine.gov.scot/datafiles/lot/hywind/Environmental_Statement/Environmental_Statement.pdf

[77] Argaut P. Underground cables. 2021:759–866. https://doi.org/10.1007/978-981-32-9938-2_10

[78] Georgallis G. Submarine cables. In: The global cable industry. Wiley; 2021. pp. 291–310. https://doi.org/10.1002/9783527822263.ch10

[79] Li C, Mogollón JM, Tukker A, Steubing B. Environmental impacts of global offshore wind energy development until 2040. Environ Sci Technol 2022;56(16):11567–77. https://doi.org/10.1021/acs.est.2c02183. https://pubs.acs.org/doi/10.1021/acs.est.2c02183

[80] Xu H, Rui S, Shen K, Jiang L, Zhang H, Teng L. Shared mooring systems for offshore floating wind farms: a review. Energy Rev 2024;3(1):100063. https://doi.org/10.1016/j.enrev.2023.100063

[81] Housner S, Hall M, Tran TT, de Miguel Para B, Maeso A. Shared mooring system designs and cost estimates for wave energy arrays. Renew Energy 2024;231:120924. https://doi.org/10.1016/j.renene.2024.120924

[82] GEBCO Compilation Group. GEBCO 2021 grid. 2021. https://doi.org/10.5285/c6612cbe-50b3-0cffe053-6c86abc09f8f. https://www.gebco.net/data_and_products/gridded_bathymetry_data/gebco_2021/

[83] Wessel P, Smith WHF. GSHHG, a global self-consistent, hierarchical, high-resolution geography database version 2.3.7. 2017. https://www.soest.hawaii.edu/pwessel/gshhg/

[84] Alday M, Lavidas G. The ECHOWAVE hindcast: a 30-years high resolution database for wave energy applications in North Atlantic European waters. Renew Energy 2024;236:121391. https://doi.org/10.1016/J.RENENE.2024.121391

[85] Alday M, Lavidas G. Data underlying the publication: the ECHOWAVE hindcast: a 30-years high resolution database for wave energy applications in North Atlantic European waters. 2024. https://doi.org/10.4121/f359cd0f-d135-416c-9118-e79dccba57b9.v1

[86] Raghavan V, Loukogeorgaki E, Mantadakis N, Metrikine AV, Lavidas G. HAMS-MREL, a new open source multiple body solver for marine renewable energies: model description, application and validation. Renew Energy 2024:121577. https://doi.org/10.1016/J.RENENE.2024.121577. https://linkinghub.elsevier.com/retrieve/pii/S0960148124016458

[87] Hersbach H, Berrisford P, Bell B, Biavati G, Horányi A, Muñoz Sabater J, et al. ERA5 hourly data on single levels from 1940 to present. 2023. https://doi.org/10.24381/cds.adbb2d47

[88] López M, Rodríguez N, Iglesias G. Combined floating offshore wind and solar PV. J Mar Sci Eng 2020;8(8):576. https://doi.org/10.3390/jmse8080576
[89] Santiago I, Trillo-Montero D, Moreno-Garcia IM, Pallarés-López V, Luna-Rodríguez JJ. Modeling of photovoltaic cell temperature losses: a review and a practice case in South Spain. Renew Sustain Energy Rev 2018;90:70–89. https://doi.org/10.1016/j.rser.2018.03.054
[90] Skoplaki E, Boudouvis AG, Palyvos JA. A simple correlation for the operating temperature of photovoltaic modules of arbitrary mounting. Sol Energy Mater Sol Cells 2008;92(11):1393–402. https://doi.org/10.1016/j.solmat.2008.05.016
[91] Aoun N. Methodology for predicting the PV module temperature based on actual and estimated weather data. Energy Conver Manag: X 2022;14:100182. https://doi.org/10.1016/j.ecmx.2022.100182
[92] vikramsolar. Spec sheet Paradea 680W. 2023. https://www.vikramsolar.com/wp-content/uploads/2022/10/Paradea_12-132-HC-2023-GG.pdf
[93] Luxor Solar. Eco line M132 HJT GG 680-700wp. 2024. https://www.luxor.solar/en/solar-modules/eco-line-gg/hjt-glass-glass-m132-680-700wp.html
[94] J. N. Energy, L. Technology Co. 680w solar panel. https://www.jingsun-power.com/solar-panel/mono-solar-panel/680w-solar-panel.html
[95] Solardrop Store. Solar panel 680 watts, Trinia Solar. https://solardropshipping.com/en/product/solar-panel-bifacial-half-cut-monocrystalline-680-w-trina-solar-3649
[96] Bak C, Zahle F, Bitsche R, Kim T, Yde A, Henriksen LC, et al. The DTU 10-MW reference wind turbine. 2013. https://orbit.dtu.dk/en/publications/the-dtu-10-mw-reference-wind-turbine
[97] Penalba M, Touzón I, Lopez-Mendia J, Nava V. A numerical study on the hydrodynamic impact of device slenderness and array size in wave energy farms in realistic wave climates. Ocean Eng 2017;142:224–32. https://doi.org/10.1016/j.oceaneng.2017.06.047. https://linkinghub.elsevier.com/retrieve/pii/S0029801817303517
[98] Bassi A, Biganzoli S, Ferrara F, Amadei N, Valente A, Sala A, et al. Updated characterisation and normalisation factors for the environmental footprint 3.1 method. https://doi.org/10.2760/798894. https://joint-research-centre.ec.europa.eu
[99] Damiani M, Ferrara N, Ardente F. Understanding product environmental footprint and organisation environmental footprint methods, EUR 31236, Tech. rep., Luxembourg: Publications Office of the European Union; 2022. https://doi.org/10.2760/11564. https://publications.jrc.ec.europa.eu/repository/handle/JRC129907
[100] GreenDelta. OpenLCA - the life cycle and sustainability modeling suite. 2024. https://www.openlca.org/openlca/
[101] Wernet G, Bauer C, Steubing B, Reinhard J, Moreno-Ruiz E, Weidema B. The ecoinvent database version 3 (part I): overview and methodology. Int J Life Cycle Assess 2016;21(9):1218–30. https://doi.org/10.1007/S11367-016-1087-8/FIGURES/7. https://link.springer.com/article/10.1007/s11367-016-1087-8
[102] Ecoinvent. Market for photovoltaic panel, single-Si wafer, GLO, allocation, cut-off, ecoinvent 3.10. 2011.
[103] Niels J. Market for photovoltaic mounting system, for 570kWp open ground module, GLO, allocation, cut-off, ecoinvent 3.10. 2012.
[104] Principle Power. Kincardine offshore wind farm. https://www.principlepower.com/projects/kincardine-offshore-wind-farm
[105] Aquatera Ltd. Mocean energy Orkney M100P test 2022 - project briefing note, Tech. rep. (2021).
[106] Aquatera Ltd, Aquatera Ltd. The Farr Point wave farm development-environmental scoping report, Tech. rep. (2011).
[107] BVG Associates. Guide to a floating offshore wind farm, Tech. rep. (2023 May) https://guidetofloatingoffshorewind.com/
[108] Wave Energy Scotland Limited. Moorings & connections: overview, description & functional spec, Tech. rep., Quoceant Ltd; 2016. https://www.waveenergyscotland.co.uk/research-strategy/knowledge-capture/knowledge-capture-pelamis-wave-power-ltd/
[109] Rinaldi G, Portillo JCC, Khalid F, Henriques JCC, Thies PR, Gato LMC, et al. Multivariate analysis of the reliability, availability, and maintainability characterizations of a spar-buoy wave energy converter farm. J Ocean Eng Mar Energy 2018;4(3):199–215. https://doi.org/10.1007/s40722-018-0116-z
[110] Ambühl S, Marquis L, Kofoed JP, Dalsgaard Sørensen J. Operation and maintenance strategies for wave energy converters. Proc Inst Mech Eng Part O J Risk Reliab 2015;229(5):417–41. https://doi.org/10.1177/1748006X15577877
[111] Wang J, Lund PD. Review of recent offshore photovoltaics development. Energies 2022;15(20):7462. https://doi.org/10.3390/en15207462
[112] Al-Sallami O. Cables decommissioning in offshore wind farms: environmental and economical perspective. 2021. https://urn.kb.se/resolve?urn=urn:nbn:se:uu:diva-448448
[113] Taormina B, Bald J, Want A, Thouzeau G, Lejart M, Desroy N, et al. A review of potential impacts of submarine power cables on the marine environment: knowledge gaps, recommendations and future directions. Renew Sustain Energy Rev 2018;96:380–91. https://doi.org/10.1016/j.rser.2018.07.026. https://linkinghub.elsevier.com/retrieve/pii/S1364032118305355
[114] Bauer C. Wind power plant construction, 2MW, offshore, moving parts, GLO, cut-off, ecoinvent database version 3.10. 2007.
[115] EuRIC aisbl. Metal recycling factsheet by EuRIC. 2020. https://circulareconomy.europa.eu/platform/en/knowledge/metal-recycling-factsheet-euric
[116] van der Meulen TH, Bastein T, Swamy SK, Saraswati N, Joustra J. Offshore wind farm decommissioning an orientation of possible economic activity in the South Holland Region and the Rotterdam Port area, Tech. rep., TNO; 2020. https://smartport.nl/wp-content/uploads/2021/01/SmPo_TNO-Offshore-windpark-decommissioningeng_final.pdf
[117] Thomson C. Carbon and energy payback of variable renewable generation, [Ph.D. thesis], University of Edinburgh; 2014. https://era.ed.ac.uk/handle/1842/8875
[118] European Environment Agency. Trends and projections in Europe 2024, Tech. rep., Luxembourg: Publications Office of the European Union; 2024. https://doi.org/10.2800/7574066
[119] Tay ZY, Venugopal V. Hydrodynamic interactions of oscillating wave surge converters in an array under random sea state. Ocean Eng 2017;145:382–94. https://doi.org/10.1016/j.oceaneng.2017.09.012
[120] Bozzi S, Giassi M, Moreno Miquel A, Antonini A, Bizzozero F, Gruosso G, et al. Wave energy farm design in real wave climates: the Italian offshore. Energy 2017;122:378–89. https://doi.org/10.1016/j.energy.2017.01.094. https://linkinghub.elsevier.com/retrieve/pii/S0360544217301019
[121] López M, Claus R, Soto F, Hernández-Garrastacho ZA, Cebada-Relea A, Simancas O. Advancing offshore solar energy generation: the HelioSea concept. Appl Energy 2024;359:122710. https://doi.org/10.1016/j.apenergy.2024.122710
[122] WECHULL+. https://www.wechull.se/
[123] Lopez J, Ricci P, Villate JL, Bahaj AS, Myers LE, Retzler C, et al. Preliminary economic assessment and analysis of grid connection schemes for ocean energy arrays. In: 3rd International Conference On Ocean Energy, 6 October, Bilbao, 2010. https://www.ocean-energy-systems.org/publications/icoe/icoe-2010/document/preliminary-economic-assessment-and-analysis-of-grid-connection-schemes-for-ocean-energy-arrays/